In Situ IRRAS Studies of NH Stretching Bands and Molecular Structures of the Monolayers of Amphiphiles Containing Amide and Amine Units at the Air−Water Interface

Kylin Liao and Xuezhong Du*

Key Laboratory of Mesoscopic Chemistry (Ministry of Education), State Key Laboratory of Coordination Chemistry, and School of Chemistry and Chemical Engineering, Nanjing University, Nanjing 210093, People's Republic of China

Received: October 12, 2008; Revised Manuscript Received: November 23, 2008

The monolayers of the amphiphiles containing amide and amine units at the air−water interface on water surface have been studied using infrared reflection absorption spectroscopy (IRRAS). Sharp NH stretching bands are observed in the monolayers of *N*-octadecanoyl-L-alanine (ALA) (at pH 3.0) and *N*-octadecyloxalamide (OXA), while no NH stretching band is clearly detected in the monolayers of octadecan-1-amine (OA) and *N*-hexadecylethane-1,2-diamine (EDA) (at pH 9.3). It is considered that the presence and absence of the NH stretching bands are related to properties of amides and amines, roles of N−H bonds in hydrogen bond donor/acceptor, and orientation of transition moment directions of NH stretching vibrations. The intermolecular hydrogen-bonding interactions between the adjacent amides of ALA and OXA induce the parallel packing of the CCC planes of corresponding alkyl chains, while the chains are uniaxially oriented in the monolayers of OA and EDA. In the presence of $CuCl_2$ in the subphase, Cu^{2+} ions coordinate to the headgroups of OA and EDA in the monolayers; moreover a new peak at 1220 cm^{-1} is observed for the EDA monolayer and assigned to the CH_2 twisting and wagging modes relevant to the ethylenediamine headgroups. The presence of the peak is related to the dehydration of the headgroups induced by the twisted tetrahedral coordination, and the coordinated headgroups undergo an orientation change with surface pressure.

Introduction

Hydrogen bonds are of particular importance in nature and in many chemistry research areas. The hydrogen bonds, such as N−H···O and N−H···N related to amide and amine units, play a crucial role in protein folding and nucleic acid base pairing. The NH stretching mode is usually used as a fingerprint of hydrogen bonds for structural analysis and molecular recognition. Hydrogen bonds are usually suppressed or less effective for specific recognition in aqueous solution since the molecules are surrounded by bulk water.[1] Realization of effective hydrogen bonds in water is especially significant due to its relevance to biological recognition.[2] Langmuir monolayers at the air−water interface have been successfully used as a simple model for the studies of molecular recognition to minimize the interference of bulk water.[3] Over the past decade, infrared reflection absorption spectroscopy (IRRAS) has emerged as one of the leading structural analyses for the monolayers at the air−water interface.[4−15] The IRRAS technique not only allows for the characterization of chain conformation/orientation and headgroup structure but also provides valuable information about molecular interaction between the monolayers and substances dissolved in the subphase. A few examples of the hydrogen-bonding networks between complementary components have been investigated at the air−water interface mostly based on the C═O stretching bands using the IRRAS technique.[12,13,16,17]

We reported the first observation of sharp NH stretching bands from the monolayers of *N*-octadecanoyl-L-alanine (ALA) containing an amide group at the air−water interface using the IRRAS technique and studied the change of hydrogen bonds in type and strength in the presence of metal ions in the subphase.[18] More recently, a sharp NH stretching band was also observed from the monolayer with fluorinated ethyl amide polar heads at the air−water interface.[19] However, no NH stretching band was clearly detected from the monolayer of nucleolipids with the cytosine headgroups at the air−water interface using the IRRAS technique in contrast to an obvious NH stretching bands for the corresponding Langmuir−Blodgett (LB) films by the infrared transmission technique.[16,17,20] In this paper, we investigate the monolayers of the amphiphiles containing amide and amine groups (1−2 units) shown in Chart 1 at the air−water interface using the IRRAS technique to give a deep insight into the relationship between the presence and absence of NH stretching bands and the molecular structures of the monolayers containing amide and amine units. The results indicate that the presence and absence of NH stretching bands are related to properties of amides and amines, roles of N−H bonds in hydrogen bond donor/acceptor, and orientation of transition moment directions of the N−H stretching vibrations for the monolayers at the air−water interface.

Experimental Section

Materials. The syntheses of ALA,[21] *N*-octadecyloxalamide (OXA)[22] and *N*-hexadecylethane-1,2-diamine (EDA)[23] were described in detail, respectively, and commercially available octadecan-1-amine (OA) was recrystallized from ethanol. The chemical reagents used were of analytical grade, and the water used was double-distilled (pH 5.6) after a deionized Milli-Q exchange. The water subphase for the ALA monolayer was

* To whom correspondence should be addressed. E-mail: xzdu@nju.edu.cn. Fax: 86-25-83317761.

10.1021/jp809038w CCC: $40.75
Published on Web 01/14/2009

adjusted to pH 3.0 by the addition of HCl, and the water subphase for the OA and EDA monolayers to pH 9.3 by the addition of NaOH. The pH of the Cu^{2+}-containing subphase ($CuCl_2$, 1 mM) was 5.3 without the addition of HCl or NaOH.

CHART 1: Chemical Structures of the Amphiphiles Containing Amide and Amine Units

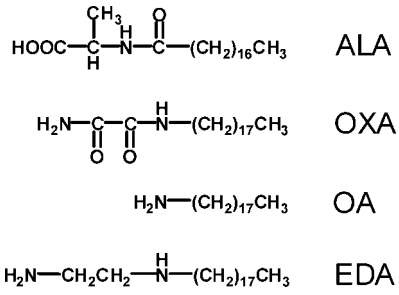

Isotherm Measurements. Surface pressure (π)-area (A) isotherms of the monolayers of the amphiphiles at the air−water interface were recorded on a Nima 611 Langmuir trough (Nima Technology, England) equipped with a computer control. The maximum available surface area was 30 cm × 10 cm and could be varied continuously by moving two Teflon barriers. A Wihelmy plate (filter paper) was used as the surface pressure sensor with an accuracy of ±0.1 mN/m and situated in the middle of the trough. Chloroform solutions of amphiphiles were spread on water surface and then 15 min was allowed for solvent evaporation. Two barriers compressed symmetrically at the same rate 5 mm/min. Each sample was run at least three times to ensure reproducibility at 22 °C.

IRRAS Spectrum Measurements. IRRAS spectra of the monolayers at the air−water interface were recorded on an Equinox 55 FTIR spectrometer (Bruker, Germany) connected to an XA-511 external reflection attachment with a shuttle trough system and a liquid-nitrogen-cooled MCT detector. Sample (film-covered surface) and reference (film-free surface) troughs were fixed on a shuttle device driven by a computer-controlled stepper motor for allowing collection from the two troughs in an alternating fashion. A KRS-5 polarizer was used to generate perpendicularly polarized infrared beams. These experiments were carried out at 22 °C. The film-forming molecules were spread from chloroform solution of desired volumes, and 20 min was allowed for solvent evaporation. The measurement system was then enclosed for humidity equilibrium and monolayer relaxation for 4 h prior to compression. The monolayers were compressed discontinuously to the desired surface pressures from ~0 mN/m. After 30 min of relaxation, the two moving barriers were stopped and the monolayer areas were kept unchanged. The external reflection absorption spectra of pure water and ion-containing solutions were used as references, respectively. The spectra were recorded with a resolution of 8 cm^{-1} by coaddition of 1024 scans. A time delay of 30 s was allowed for film equilibrium between the trough movement and data collection. The spectra were acquired using p-polarized beam followed by data collection using s-polarized one. The IRRAS spectra were presented without smoothing or baseline correction.

Results and Discussion

Isotherms of the Monolayers on Pure Water. Figure 1 shows $\pi-A$ isotherms of the different monolayers on pure water subphase. The OA monolayer exhibits typical condensed characteristics with a limiting area of 0.19 nm^2/molecule and a collapse pressure of more than 70 mN/m at pH 9.3, which indicates that the OA molecules in the condensed monolayer are oriented almost perpendicular to the water surface. The EDA monolayer displays the feature of considerable expansion with a limiting area of 0.336 nm^2/molecule (at pH 9.3); even some of the amphiphiles could dissolve into the subphase at higher surface pressures. The ALA molecules form a condensed monolayer on pure water (at pH 3.0) with a limiting area of 0.256 nm^2/molecule and a collapse pressure of ca. 45 mN/m, after which the monolayer is collapsed upon further compression. The OXA isotherm shows extremely condensed characteristics with a limiting area of 0.102 nm^2/molecule, much smaller than the cross-sectional area (about 0.2 nm^2) of a saturated hydrocarbon chain and the limiting area of ALA. The similar cases were observed previously for the *N*-hexadecanoylalanine monolayers in the presence of Pb^{2+} or Zn^{2+} in the subphase.[6] It was considered to be due to the formation of three-dimensional structures of the compressed monolayers.[6]

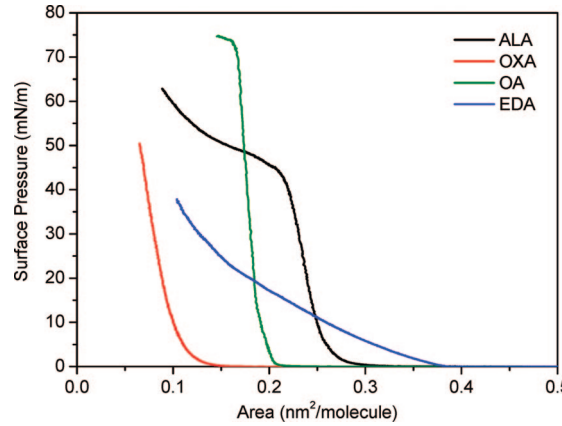

Figure 1. Surface pressure−area isotherms of the monolayers of ALA (pH 3.0), OXA (pH 5.6), OA (pH 9.3), and EDA (pH 9.3) on pure water.

NH Stretching Bands Observed from the Monolayers. IRRAS data are defined as plots of reflectance-absorbance (RA) versus wavenumber. RA is defined as $-\log(R/R_0)$, where R and R_0 are the reflectivities of the film-covered and film-free surfaces, respectively. The selection rules of the IRRAS for the monolayers at the air−water interface[4] are first presented. For s-polarization, the electric field vector is perpendicular to the plane of incidence, that is, parallel to the water surface. The bands are always negative and their intensities decrease with increasing angle of incidence. For p-polarization, the electric field vector is parallel to the plane of incidence. For the vibrations with their transition moments parallel to the water surface, the bands are initially negative and their intensities increase with increasing angle of incidence to reach a maximum, then a minimum in the reflectivity is found at the Brewster angle. Above the Brewster angle, the bands become positive and their intensities decrease upon further increase of incidence angle. For the vibrations with their transition moments perpendicular to the water surface, the bands are positive first and then become negative above the Brewster angle.[10,24] If the vibrational transition moments are tilted to the air−water interface, the intensities of the bands are weak and even zero.[25]

Figure 2 shows the p-polarized IRRAS spectra of the different monolayers on water subphase at various surface pressures, and the corresponding s-polarized spectra are presented in Figure S1 in the Supporting Information. The spectral bands and their assignments for the monolayers are listed in Table 1. The IRRAS spectra of the ALA monolayers at 5−20 mN/m were described

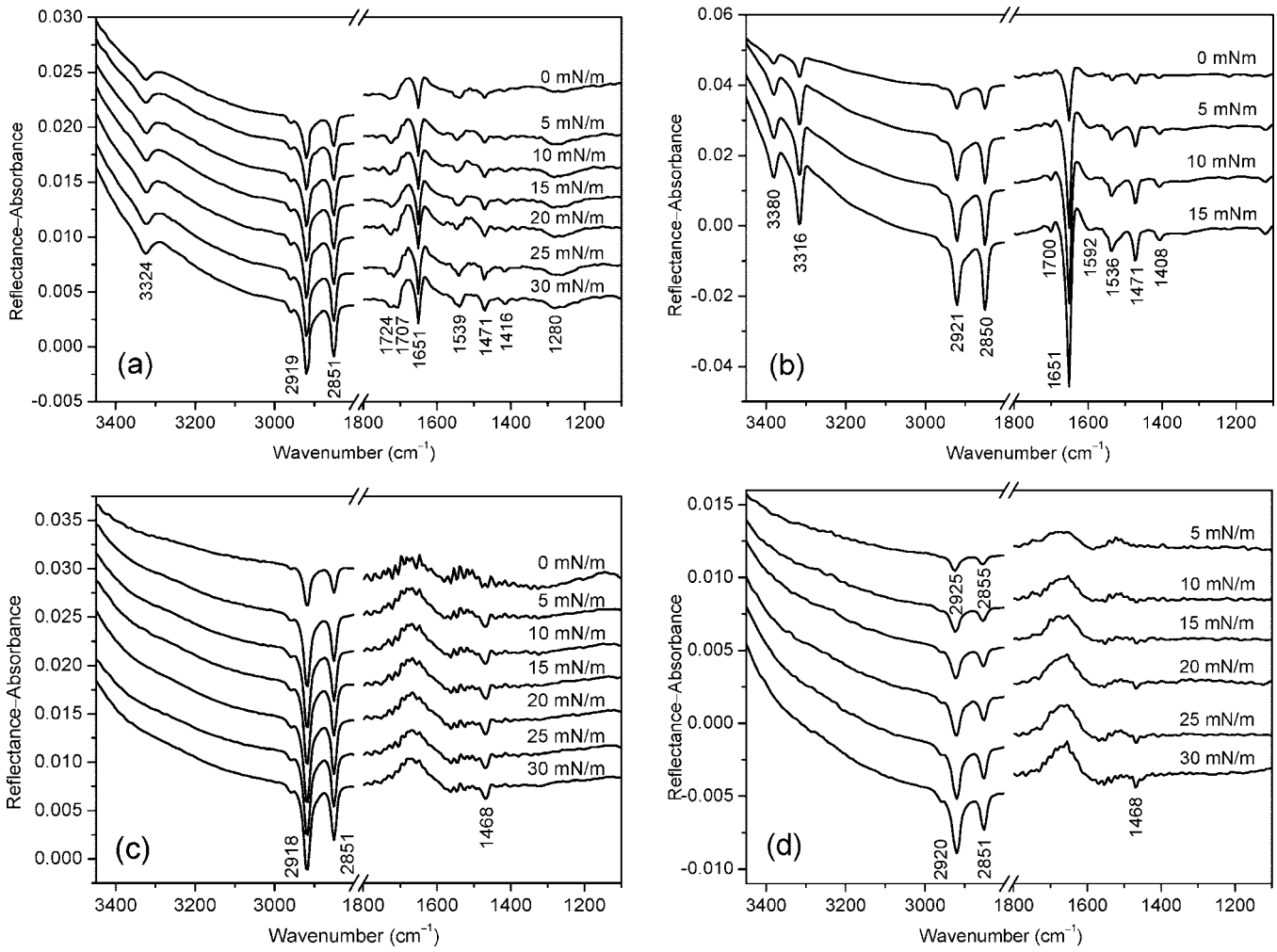

Figure 2. p-Polarized IRRAS spectra of the monolayers on pure water at different surface pressures at an incidence angle of 30°. (a) ALA (pH 3.0); (2) OXA (pH 5.6); (3) OA (pH 9.3); (4) EDA (pH 9.3).

TABLE 1: IRRAS Bands and Their Assignments for the Different Monolayers at the Air-Water Interface[a]

wavenumber (cm^{-1})				
ALA	OXA	OA	EDA	assignment
	3380			$\nu_a(NH_2)$
3324	3315			ν(NH)
2919	2921	2918	2925−2920	$\nu_a(CH_2)$
2851	2850	2851	2855−2851	$\nu_s(CH_2)$
1724, 1707				ν(C═O) in COOH
	1700			ν(C═O) in primary amide
1651	1651			ν(C═O) in secondary amide
	1594			$\delta(NH_2)$ in primary amide
1539	1537			δ(NH) + ν(CN) in secondary amide
1471	1471	1468	1468	$\delta(CH_2)$
1416	1406			
1280				ν(CN) in secondary amide
	1120			$\rho(NH_2)$

[a] ν, stretching vibration; ν_a, antisymmetric stretching vibration; ν_s, symmetric stretching vibration; δ, deformation vibration; ρ, rocking vibration.

in detail previously.[18] Seen from Figure 2a, the sharp NH stretching bands at 3324 cm^{-1} are observed from the monolayers not only at 5−30 mN/m but also even at 0 mN/m. All of the bands at 0 mN/m almost have the same frequencies as those at 30 mN/m, and the $\nu_a(CH_2)$ and $\nu_s(CH_2)$ bands appear at 2919 and 2851 cm^{-1}, respectively, indicative of ordered conformation of alkyl chains.[26] The singlet $\delta(CH_2)$ peak at 1471 cm^{-1} indicates that the alkyl chains are in a triclinic subcell where the adjacent CCC planes are packed in a parallel fashion.[27] This is because the parallel chain arrangement is favorable to the intermolecular N−H···O═C hydrogen bonds between the adjacent amide groups.

It is well known that the formation of hydrogen bonds shifts the ν(NH) and ν(C═O) bands to lower wavenumbers and repositions the δ(NH) peak in the opposite direction.[28] For open-chain secondary amides, the trans isomers with opposite orientation of N−H and C═O bonds expose the free ν(NH) peak at 3460−3400 cm^{-1}, and hydrogen-bonded trans NH groups exhibit the ν(NH) peak at 3320−3270 cm^{-1}.[19,28] The ν(NH) bands at 3324 cm^{-1} in Figure 2a indicate that the N−H···O═C hydrogen bonds are formed between the adjacent secondary amides for a lateral intermolecular network. In the corresponding LB films, the ν(NH) bands were also observed at 3324 cm^{-1}, and the order−disorder phase transition of the LB films occurred at the temperature as high as 122 °C owing to the intermolecular hydrogen-bonding interaction.[29] In addition, the frequency position of amide II band at 1539 cm^{-1} also supports the occurrence of the hydrogen-bonding interaction in comparison to the free amide II band at 1510 cm^{-1}.[30]

OXA might be regarded to have a secondary amide and a primary amide. The two sharp bands at 3380 and 3315 cm^{-1} in Figure 2b are attributed to the $\nu_a(NH_2)$ vibration of the primary amide and the ν(NH) one of the secondary amide, respectively.[31,32]

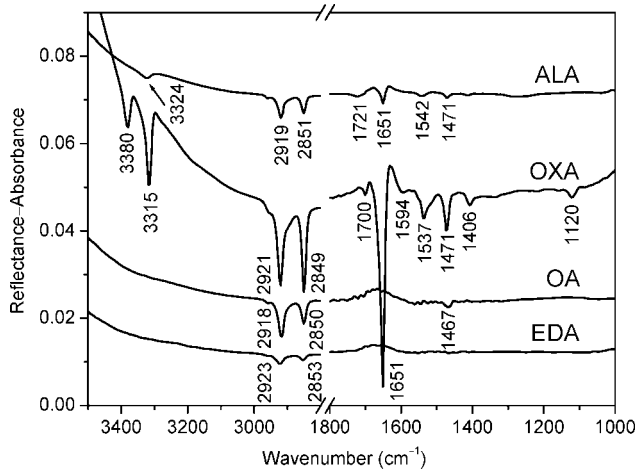

Figure 3. p-Polarized IRRAS spectra of the monolayers on pure water at the surface pressure of 15 mN/m at an incidence angle of 30°.

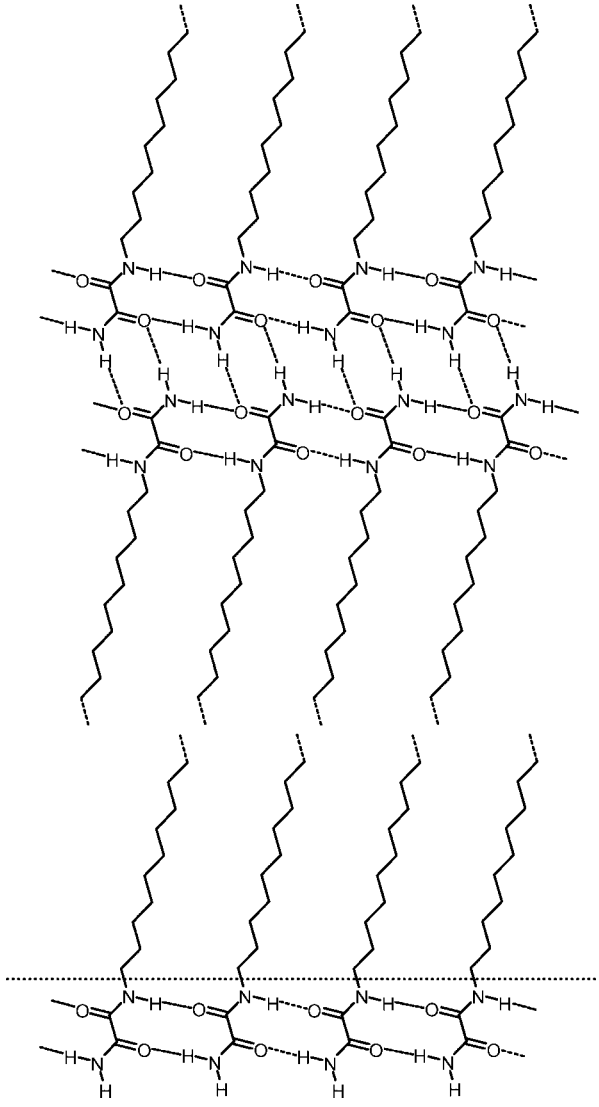

Figure 4. Schematic representation of the intralayer and interlayer hydrogen-bonded networks in the three-dimensional structures of the compressed monolayers of OXA on pure water.

Considering the frequency positions of the ν(NH)/ν_a(NH_2), amide I, and amide II bands, it is obvious that the primary amides and secondary amides are involved in the hydrogen-bonding interactions, respectively. On the other hand, the

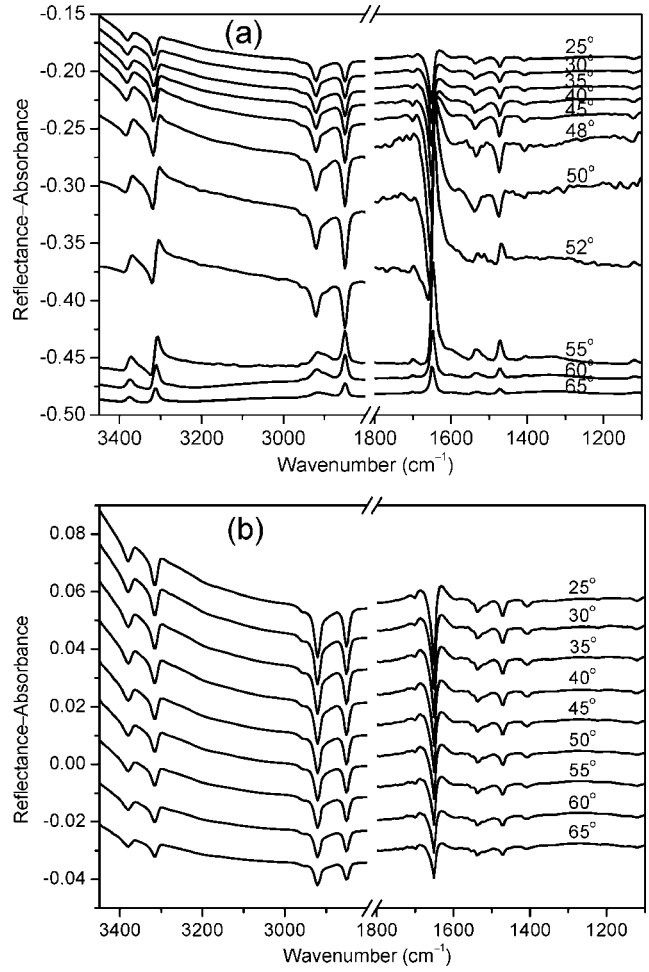

Figure 5. IRRAS spectra of the OXA monolayers on pure water at the surface pressure of 15 mN/m against angle of incidence. (a) p-polarization; (b) s-polarization.

ν_s(CH_2) band intensities are stronger than the ν_a(CH_2) ones at different surface pressures. This behavior reflects that the adjacent CCC planes of the hydrocarbon chains are preferentially oriented parallel to the water surface.[24] Further analysis of chain orientation is presented in the following (see the next subsection).

However, no sharp ν(NH)/ν_a(NH_2) peak can be observed from the monolayers of OA and EDA at various surface pressures (Figure 2c,d). In the case of OA, the ν_a(CH_2) and ν_s(CH_2) bands appear at 2918 and 2851 cm^{-1}, respectively, irrespective of surface pressure, indicating that the alkyl chains take ordered conformations even in the vicinity of 0 mN/m. While in the case of EDA, the two bands decrease in frequency from 2925 and 2855 cm^{-1} to 2920 and 2851 cm^{-1}, respectively, with the increase of surface pressure from 5 to 30 mN/m, indicating an increase in chain order from highly disordered conformations to ordered ones with surface pressure. The changes in chain order for the two monolayers on the molecular level are basically consistent with the "macroscopic information" from the corresponding isotherms. The δ(CH_2) peaks for the OA monolayers at various surface pressures and for the EDA monolayers at high surface pressures are present at 1468 cm^{-1}, which indicates that the alkyl chains are packed in a hexagonal subcell in these cases.[33] Obviously, the chain packing in the monolayers containing amine groups is different from that in the monolayers containing amide groups.

The sharp ν(NH)/ν_a(NH_2) bands can be clearly observed in the ALA and OXA monolayers containing (primary and

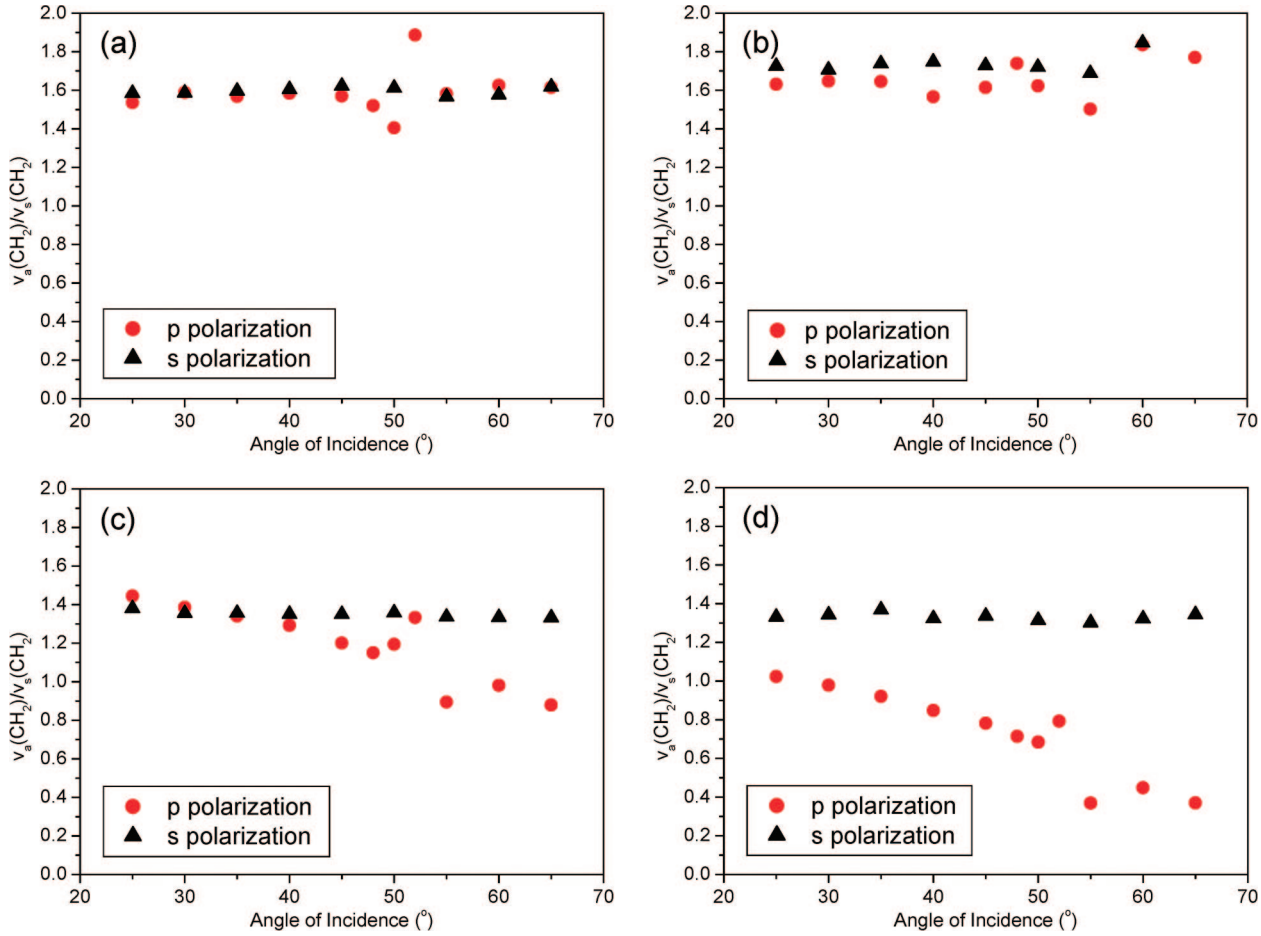

Figure 6. Ratios of $\nu_a(CH_2)$ band intensity to $\nu_s(CH_2)$ one for the monolayers of ALA, OXA, OA, and EDA at the air−water interface as a function of incidence angle for p- and s-polarization. (a) OA; (b) EDA; (c) ALA; (d) OXA.

secondary) amide groups but not in the OA and EDA monolayers containing amine ones. A few probable reasons are analyzed in the followings. First, the properties of the N−H bonds in amides are different from those in amines. Generally, the ν(NH) bands from amide groups are stronger than those from amine ones. Second, the free pair of electrons that is available in an amino function for hydrogen bond formation is not available in an amide function because of its distribution in the complete mesomeric system. That means that the N−H bonds in amides cannot act as hydrogen acceptors effectively, while the N−H bonds in amines are both hydrogen donors and hydrogen acceptors, which results in the weakening and broadening of the probable ν(NH) bands particularly at the air−water interface, so that no ν(NH) band can be obviously observed. It is well known that amines are readily protonated in aqueous environments. In our previous work,[16,17] no ν(NH) band was clearly observed in the IRRAS spectra of the monolayers of 1-(2-octadecyloxycarbonylethyl)cytosine at the air−water interface, while obvious ν(NH) bands appeared in the FTIR transmission spectra of the corresponding LB films.[16,17,20] The trans-isomer amides are easy to form intermolecular N−H···O═C hydrogen bonds to prevent them from contacting with subphase water and to suppress the interaction with water molecules. Third, the presence and absence of the ν(NH)/$\nu_a(NH_2)$ bands are also correlated with the orientation of their vibrational transition moments. The N−H bonds in the secondary amides involved in intermolecular hydrogen-bonded network in the monolayers are preferentially oriented parallel to the water surface, and the $\nu_a(NH_2)$ transition moments in the primary amides are tilted to some degree with respect to the monolayer normal. In the case of OXA, the ν(NH) band is stronger than the $\nu_a(NH_2)$ one. In the OA and EDA monolayers, the intermolecular hydrogen-bonding interactions may be formed both between the adjacent amines and between the amines and water molecules, so that the ν(NH) and $\nu(NH_2)$ transition moments are oriented at different angles or mostly tilted relative to the monolayer normal, which would result in weakening or absence of corresponding bands.[25]

Figure 3 compares the IRRAS spectra of the different monolayers at the air−water interface at 15 mN/m. Of note is that all of the bands are considerably intensified in the case of OXA. This is related to the occurrence of the three-dimensional structures of the compressed monolayers, which is consistent with the extremely condensed characteristics of the corresponding isotherm. Luo et al. reported the formation of organogels from OXA in a variety of nonpolar or low polar organic solvents and found that the presence of the primary amide (neither of two hydrogen atoms was substituted) was a necessary for the formation of interlayer hydrogen bonds between the head-to-head arrangements in the organogels.[22] A schematic illustration of the probable three-dimensional structures of OXA at the air−water interface with intralayer and interlayer hydrogen bonds is shown in Figure 4. However in the case of EDA, the $\nu_a(CH_2)$, and $\nu_s(CH_2)$ bands appear at 2923 and 2853 cm^{-1} and are very weak in comparison with the other monolayers, indicating that lots of gauche conformers are populated in the alkyl chains.

Chain Packing and Orientation in the Monolayers. Figure 5 shows p- and s-polarized IRRAS spectra of the OXA multilayers at 15 mN/m against angle of incidence. For

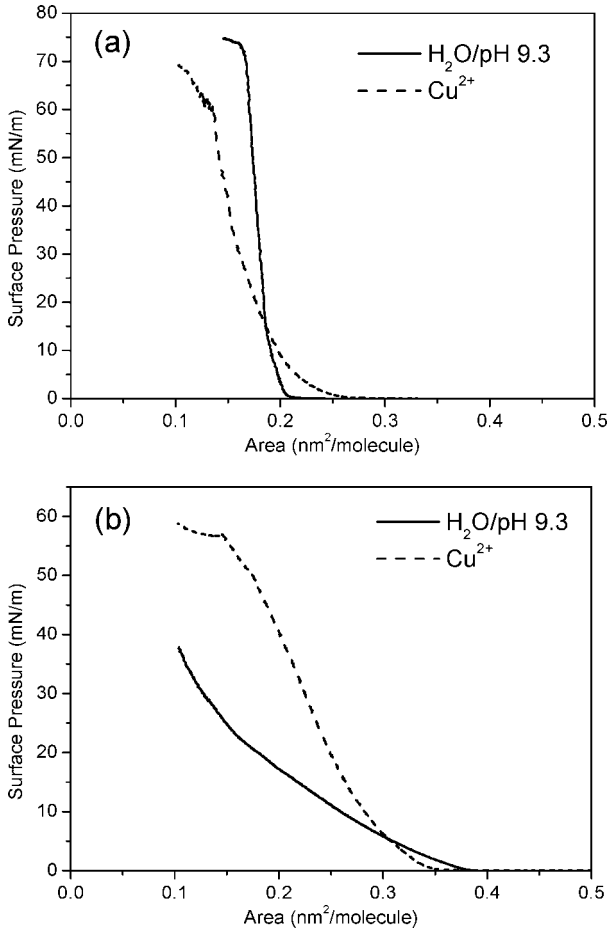

Figure 7. Surface pressure−area isotherms of the monolayers on pure water and the Cu^{2+}-containing subphase. (a) OA; (b) EDA.

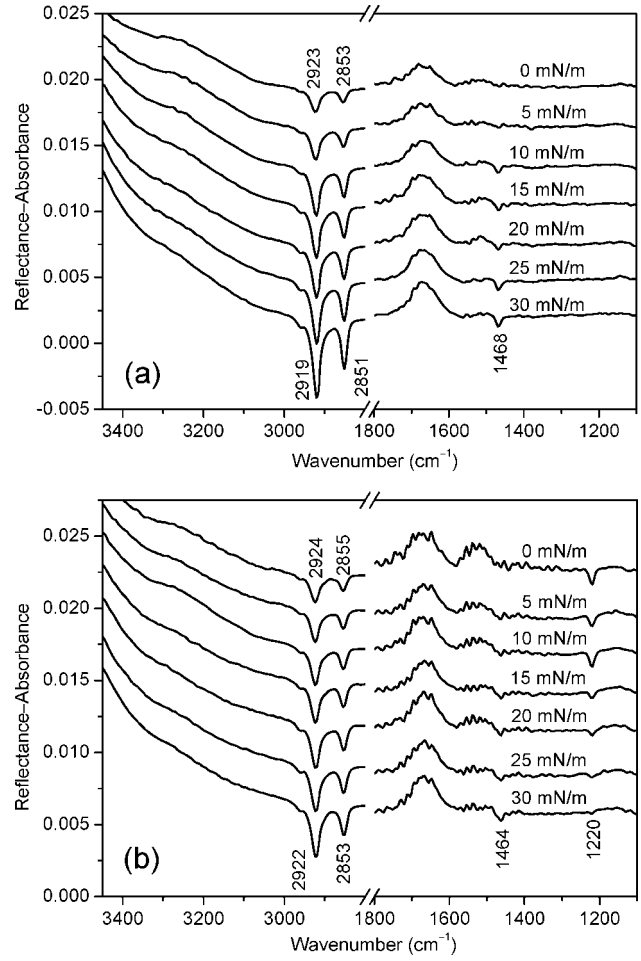

Figure 8. p-Polarized IRRAS spectra of the monolayers on the Cu^{2+}-containing subphase at different surface pressures at an incidence angle of 30°. (a) OA; (b) EDA.

p-polarization, the $\nu_a(CH_2)$ band intensities are almost smaller than the $\nu_s(CH_2)$ ones in the range of the incidence angles investigated below and above the Brewster angle, so that the intensity ratio of $\nu_a(CH_2)$ to $\nu_s(CH_2)$ bands $[\nu_a(CH_2)/\nu_s(CH_2)]$ is reduced to be smaller than 1. The extent of the increase in the $\nu_s(CH_2)$ band intensity is more than that in the $\nu_a(CH_2)$ one with increasing angle of incidence. Beyond the Brewster angle, the two bands become positive, but the $\nu_a(CH_2)$ band intensity is considerably reduced in comparison with the $\nu_s(CH_2)$ one. The corresponding spectra of the other monolayers against angle of incidence are shown in Supporting Information, Figures S2−S4.

Figure 6 shows intensity ratios of $\nu_a(CH_2)/\nu_s(CH_2)$ for the different monolayers on water subphase at various angles of incidence for p- and s-polarization, respectively. The intensity ratio of $\nu_a(CH_2)/\nu_s(CH_2)$ reflects the preferential orientation of the CCC planes of hydrocarbon chains, and the s-polarized IRRAS technique is not as sensitive to the preferential orientation of hydrocarbon chains as the p-polarized one.[10] In the cases of OA and EDA, the intensity ratios remain almost unchanged around a value of 1.6−1.7, independent of angle of incidence for p- and s-polarization but a little fluctuation near the Brewster angle for p-polarization. These characteristics indicate that the hydrocarbon chains in the monolayers are uniaxially oriented with respect to the surface normal.[34] In the case of ALA and OXA, the intensity ratios for s-polarization are around 1.3−1.4 irrespective of angle of incidence, while the ratios for p-polarization nearly take a gradual decrease with increasing angle of incidence, particularly in the case of OXA. These indicate that the hydrocarbon chains in the cases of ALA and OXA have a different orientation feature from the uniaxial orientation in the cases of OA and EDA.

It is well known that both methylene transition moment directions are perpendicular to the alkyl chains, with the $\nu_s(CH_2)$ transition moment being oriented along the bisector of the methylene H−C−H bond angle, while the $\nu_a(CH_2)$ transition moment is perpendicular to this. For p-polarization, a methylene stretching band intensity will become maximal, when all transition moments are oriented horizontally, that is, the alkyl chains are perpendicular to the water surface. The spectral changes indicate that the CCC planes of the alkyl chains are preferentially oriented parallel to the water surface, together with the $\nu_s(CH_2)$ transition moments parallel to the water surface and the $\nu_a(CH_2)$ ones perpendicular to the water surface more or less. The apparent reduction in the $\nu_a(CH_2)$ intensity results from the contribution of the band components of opposite signs with the directional transition moments oriented along the surface normal.[17,24] It is clear that the preferential orientation of the alkyl chains is closely related to the formation of hydrogen bonds between the amide groups of the adjacent amphiphiles.

OA and EDA Monolayers on Cu^{2+}-containing Subphase. The N atoms in amines cannot only act as proton acceptors but also coordinate to transition metal ions. Figure 7 shows $\pi-A$ isotherms of the OA and EDA monolayers on Cu^{2+}-containing subphases in comparison with those on pure water (at pH 9.3). In the case of OA, the monolayer in the presence of Cu^{2+} displays a little expansion at low surface pressures and slight condensation at high surface pressures. The corresponding

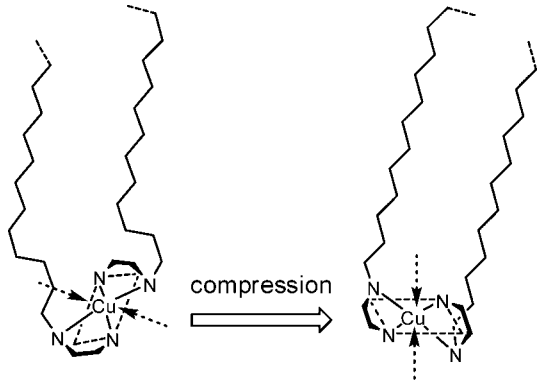

Figure 9. Schematic illustration of the twisted tetrahedral coordination of the EDA headgroups and orientation change with surface pressure in the monolayers in the presence of Cu^{2+}.

IRRAS spectra (Figure 8a) indicate that the alkyl chains undergo a change from disordered conformations to ordered ones with surface pressure, which is different from the ordered conformations of the alkyl chains at various surface pressures on pure water (Figure 2c). In the case of EDA, a stable monolayer is formed in the presence of Cu^{2+} with a limiting area of ca. 0.3 nm^2 and a collapse pressure of more than 50 mN/m, and the monolayer exhibits expanded characteristics at most of surface pressures in comparison with that on pure water. The corresponding IRRAS spectra (Figure 8b) indicate that the alkyl chains are mostly in the disordered conformations at different surface pressures. Interestingly, a new peak at 1220 cm^{-1} is clearly observed in the presence of Cu^{2+}, and the intensity is reduced with increasing surface pressure for p-polarization so that the peak is almost absent at 30 mN/m. The difference in isotherm and IRRAS spectrum between the monolayers on pure water and the Cu^{2+}-containing subphase indicate that the EDA headgroups coordinate with Cu^{2+} ions. For asymmetric derivatives of ethylenediamine, the ML2-type complexes of Cu^{2+}-coordinated amphiphiles usually have CuN_4 structures with cis and trans isomers.[35] Liang and co-workers reported the formation of coordinated vesicles from EDA and its homologues in aqueous Cu^{2+} solutions and confirmed that in aqueous $CuCl_2$ solution the Cu^{2+}-coordinated EDA headgroups adopted a trans-configuration twisted tetrahedral coordination CuN_4.[36] Similarly, the same metal coordination may occur for the EDA monolayers at the air−water interface on the aqueous $CuCl_2$ solution.

It is shown that the crystal of linear poly(ethylene imine) (PEI) exhibits double-stranded-helix structures in a dry state and planar zigzag structures in a hydrated state.[37] Water molecules are considered to play a key role to cause the structural change. In the case of EDA, the metal coordination may weaken or even eliminate hydration effect of the ethylenediamine headgroups in the monolayers, and the EDA headgroups of twisted tetrahedral coordination might be regarded as a small fraction (or a repeating unit) of the double-stranded-helix structures of PEI in the dry state. A band at 1247 cm^{-1} in the case of PEI was attributed to the mixed mode of the CH_2 wagging and twisting vibrations according to Hashida et al.,[38] and the directions of the transition moments of the two modes have been confirmed to be nearly the same as each other and are oriented almost parallel to the PEI chain axis.[39] Recent analysis of normal modes by the use of the density functional theory (DFT) calculation has indicated that the band is governed by the CH_2 twisting vibration.[39] Herein, the peak at 1220 cm^{-1} observed from the EDA monolayers in the presence of Cu^{2+} is tentatively assigned to the mixed mode of the CH_2 twisting and wagging vibrations relevant to the ethylenediamine headgroups. The decrease in frequency may result from the induction of metal coordination in comparison to the 1247 cm^{-1} band in the case of dry PEI.[38] To date, the IRRAS bands in the range of 1300−1100 cm^{-1} relevant to the CH_2 vibrations of hydrocarbon chains at the air−water interface have not been clearly observed. It was reported that the dip-coated films of PEI on the germanium substrates underwent a structural transition from the doubled-stranded-helix structure in a dry condition to the planar zigzag structure in a hydrated condition.[39] The 1247 cm^{-1} band was obviously observed in the dry condition with the direction of the transition moment preferentially perpendicular to the substrate surface and was absent in the hydrated condition.[39] Comparatively, a probable reason that the peak is not observed in the EDA monolayers on pure water is because that the structures of the ethylenediamine headgroups are different from those of the twisted tetrahedral coordination on the Cu^{2+}-containing subphase. For p-polarization, the decrease of the band intensity at 1220 cm^{-1} with surface pressure in the case of Cu^{2+} is due to the change of the transition moment direction from almost parallel to the water surface to favorably perpendicular to the surface. This means that the headgroups of twisted tetrahedral coordination undergo a change in orientation for optimal chain packing with surface pressure. The twisted tetrahedral coordination of the EDA headgroups and orientation change with surface pressure are schematically represented in Figure 9.

Conclusions

In summary, sharp NH stretching bands are observed in the monolayers of ALA and OXA containing amide units, while no NH stretching band is obviously detected in the monolayers of OA and EDA containing amine units. The presence and absence of the NH stretching bands are considered to be related to properties of amides and amines, roles of N−H bonds in hydrogen bond donor/acceptor, and orientation of transition moment directions of NH stretching vibrations. The intermolecular hydrogen-bonding interactions between the adjacent amides of ALA and OXA induce the orientation of the CCC planes of corresponding alkyl chains parallel to the water surface, while the chains are uniaxially oriented in the monolayers of OA and EDA with respect to the monolayer normal. In the presence of $CuCl_2$ in the subphase, Cu^{2+} ions coordinate to the headgroups of OA and EDA in the monolayers, and a new peak at 1220 cm^{-1} is observed for the EDA monolayer. The peak is attributed to the CH_2 twisting and wagging modes relevant to the ethylenediamine headgroups. The presence of the peak is due to the dehydration of the headgroups induced by the twisted tetrahedral coordination, and the coordinated headgroups undergo an orientation change with surface pressure.

Acknowledgment. The work was supported by the National Natural Science Foundation of China (Grants 20673051, 20635020, and NFFTBS J0630425), the Natural Science Foundation of Jiangsu Province (Grant BK2007519), and the program for New Century Excellent Talents in University (NCET-07-0412).

Supporting Information Available: s-Polarized IRRAS spectra of the monolayers of ALA, OXA, OA, and EDA on pure water at different surface pressures and IRRAS spectra of the monolayers of ALA, OA, and EDA on pure water at the surface pressure of 20 mN/m against angle of incidence for p- and s-polarization. This material is available free of charge via the Internet at http://pubs.acs.org.

References and Notes

(1) Fersht, A. R. *Trends Biochem. Sci.* **1987**, *12*, 301.
(2) Ariga, K.; Kunitake, T. *Acc. Chem. Res.* **1998**, *31*, 371.
(3) Leblanc, R. M. *Curr. Opin. Chem. Biol.* **2006**, *10*, 529.
(4) Mendelsohn, R.; Brauner, J. W.; Gericke, A. *Annu. Rev. Phys. Chem.* **1995**, *46*, 305.
(5) Gericke, A.; Hühnerfuss, H. *Langmuir* **1994**, *10*, 3782.
(6) Hühnerfuss, H.; Neumann, V.; Stine, K. J. *Langmuir* **1996**, *12*, 2561.
(7) Hoffmann, F.; Hühnerfuss, H.; Stine, K. J. *Langmuir* **1998**, *14*, 4525.
(8) Grandbolis, M.; Desbat, B.; Blaudez, D.; Salesse, C. *Langmuir* **1999**, *15*, 6594.
(9) Brauner, J. W.; Flash, C. R.; Xu, Z.; Bi, X.; Lewis, R. N. A. H.; McElhaney, R. N.; Gericke, A.; Mendelsohn, R. *J. Phys. Chem. B* **2003**, *107*, 7202.
(10) Ren, Y.; Kato, T. *Langmuir* **2002**, *18*, 6699.
(11) Ren, Y.; Hossain, M. M.; Iimura, K.-I.; Kato, T. *J. Phys. Chem. B* **2001**, *105*, 7723.
(12) Weck, M.; Fink, R.; Ringsdorf, H. *Langmuir* **1997**, *13*, 3515.
(13) Huo, Q.; Dziri, L.; Desbat, B.; Russell, K. C.; Leblanc, R. M. *J. Phys. Chem. B* **1999**, *103*, 2929.
(14) Flash, C. R.; Gericke, A.; Mendelsohn, R. *J. Phys. Chem. B* **1997**, *101*, 58.
(15) Flash, C. R.; Gericke, A.; Keough, K. M. W.; Mendelsohn, R. *Biochim. Biophys. Acta* **1999**, *1416*, 11.
(16) Miao, W.; Du, X.; Liang, Y. *J. Phys. Chem. B* **2003**, *107*, 13636.
(17) Wang, Y.; Du, X.; Miao, W.; Liang, Y. *J. Phys. Chem. B* **2006**, *110*, 4914.
(18) Du, X.; Liang, Y. *J. Phys. Chem. B* **2004**, *108*, 5666.
(19) Andreeva, T. D.; Petrov, J. G.; Brezesinski, G.; Möhwald, H. *Langmuir* **2008**, *24*, 8001.
(20) Miao, W.; Du, X.; Liang, Y. *Langmuir* **2003**, *19*, 5389.
(21) Du, X.; Shi, B.; Liang, Y. *Langmuir* **1998**, *14*, 3631.
(22) Luo, X.; Li, C.; Liang, Y. *Chem. Commun.* **2000**, 2091.
(23) Lu, X.; Zhang, Z.; Liang, Y. *Langmuir* **1996**, *12*, 5501.
(24) Du, X.; Liang, Y. *J. Phys. Chem. B* **2005**, *109*, 7428.
(25) Wang, C.; Zheng, J.; Oliveira, O. N., Jr.; Leblanc, R. M. *J. Phys. Chem. C* **2007**, *111*, 7826.
(26) Snyder, R. G.; Hsu, S. L.; Krimm, S. *Spectrochim. Acta, Part A* **1978**, *34*, 395.
(27) Holland, R. F.; Nielsen, J. R. *J. Mol. Spectrosc.* **1962**, *9*, 436.
(28) Bellamy, L. J. *The Infrared Spectra of Complex Molecules*, 2nd ed.; John Wiley & Sons: New York, 1958; Chapter*12*.
(29) Du, X.; Liang, Y. *J. Phys. Chem. B* **2000**, *104*, 10047.
(30) Clegg, R. S.; Hutchison, J. E. *Langmuir* **1996**, *12*, 5239.
(31) Scott, T. A., Jr.; Wagner, E. L. *J. Chem. Phys.* **1959**, *30*, 465.
(32) Chouteau, J. *Bull. Soc. Chim. Fr.* **1953**, 1148.
(33) Cameron, D. G.; Casal, H. L.; Gudgin, E. F.; Mantsch, H. H. *Biochim. Biophys. Acta* **1980**, *596*, 463.
(34) Wang, Y.; Du, X.; Guo, L.; Liu, H. *J. Chem. Phys.* **2006**, *124*, 134706.
(35) Kennedy, B. P.; Lever, A. B. P. *J. Am. Chem. Soc.* **1973**, *95*, 6907.
(36) Li, C.; Lu, X.; Liang, Y. *Langmuir* **2002**, *18*, 575.
(37) Chatani, Y.; Tadokoro, H.; Saegusa, T.; Ikeda, H. *Macromolecules* **1981**, *14*, 315.
(38) Hashida, T.; Tashiro, K.; Aoshima, S.; Inaki, Y. *Macromolecules* **2002**, *35*, 4330.
(39) Kakuda, H.; Okada, T.; Hasegawa, T. *J. Phys. Chem. B* **2008**, *112*, 12940.

JP809038W